Aramid-Short-Fiber Reinforced Rubber as a Tire Tread Composite

Mehdi Razzaghi Kashani

Polymer Engineering Group, Chemical Engineering Department, Tarbiat Modares University, Tehran, Iran

Received 10 May 2008; accepted 11 January 2009
DOI 10.1002/app.30026
Published online 8 April 2009 in Wiley InterScience (www.interscience.wiley.com).

ABSTRACT: Mechanical and dynamic-mechanical properties of a typical tire tread compound reinforced with one part aramid short fibers were investigated in order to predict the effects of fibers on tire tread performances such as rolling resistance and traction. Rubber processing, including mixing and extrusion, was performed in an industrial scale. Fiber orientation as a result of extrusion was evaluated quantitatively and qualitatively using mechanical anisotropy in swelling and scanning electron microscopy, respectively. Unidirectional tensile tests revealed higher modulus, but slightly lower strength and elongation at break for the composites stretched in the longitudinal (orientation) and transverse directions than those for the isotropic reference compound with no fiber. Dynamic mechanical thermal analysis showed that relative values of loss factor for the longitudinal and transverse composites and the reference compound depended on the state of polymer as glassy or rubbery. Therefore, a high loss factor at lower temperatures and a low loss factor at higher temperatures predicted a balanced improvement of tire traction and rolling resistance as a result of fiber addition. Heat build-up and abrasion experiments showed that addition of fiber did not deteriorate other performances of tire tread. Also, the fibers had negligible effects on processing and vulcanization characteristics of the composite. J Appl Polym Sci 113: 1355–1363, 2009

Key words: Aramid short fibers; tire tread compound; dynamic-mechanical-thermal properties; rolling resistance; traction

INTRODUCTION

Investigations on short fiber–rubber composites to attain unique mechanical properties in rubber parts such as hoses and belts have been performed extensively.[1–6] It was shown that proper application of short fibers in rubber composites depends on several factors such as structural aspect ratio and orientation of fibers in the final part, strong interfacial bonding between fiber and rubber matrices, proper dispersion of fibers, and a balanced processability/stiffness/flexibility relationship for the products.[1] However, mechanical reinforcement obtained in these systems through laboratory processing techniques is frequently not achievable in conventional fabrication operations.[7] In more recent works, nylon short fibers were employed in different rubber matrices such as natural rubber (NR), acrylonitrile-butadiene rubber (NBR), and styrene-butadiene rubber (SBR),[8–10] and it was shown that modulus, tear strength, abrasion resistance, and heat build-up of the rubber compound increase by the addition of short fibers. However, elongation at break in uniaxial extension reduces in all cases, which has been considered as an indication of fiber–rubber adhesion.[2,11] Also, the degree of swelling decreases markedly with the addition of fibers,[12] and it has been shown that restricted equilibrium swelling can be used as a true measure of adhesion between short fibers and rubber.[13] However, the increase in tensile strength depends on the rubber matrix and fiber content. In the case of natural rubber, a marked minimum was observed in tensile strength of the composite containing 10 phr nylon fiber, after which it increased with the fiber content.[8] The behavior of tensile strength reduction at low fiber concentration has been observed in composites of SBR/aramid short fibers (at about 5 wt %)[14] and thermoplastic elastomer polyurethane and aramid fibers (at about 7 w%).[15] This behavior has been attributed to the dilution of particulate reinforcing fillers used in these composites.[1,14]

Study of short fiber–rubber composite is not limited to synthetic fibers, and for environmental purposes natural fibers such as cellulose, glass, carbon, coir, sisal, isora, and bamboo have been employed in NR, SBR, and tire compounds in more recent studies.[16–23] Mechanical reinforcement of rubber, as explained for synthetic fibers, was observed in these composites, but application of surface modifiers to promote fiber–rubber adhesion has been more

Correspondence to: M. R. Kashani (mehdi.razzaghi@modares.ac.ir).

emphasized with natural fibers. In a comparative study, aramid, glass, and cellulose short fibers were added to NR, SBR, and EPDM elastomers, and most enhancement in mechanical properties such as tensile strength and modulus, hardness, tear and abrasion resistance were obtained with high (10% and 20%) loading of aramid fibers.[24] However, elasticity of such composites, especially the ones filled with aramid short fibers, decreased. This led to reduction of rebound resilience and increase of compression set in these composites.[24] The same study shows that at such high loadings of short fibers, especially aramid, the scorch and cure times decrease due to higher cure rate of the compound in the presence of fibers. Degree of fiber orientation has a major effect on the properties of short fiber–rubber composites, with major gain in composites containing longitudinally oriented fibers if proper fiber–rubber interfacial bonding exists.[25,26]

Dynamic-mechanical analysis of short fiber-filled elastomers has shown that both storage and loss moduli of the composite are higher than those for unfilled elastomers, and this effect is most pronounced in the direction of fiber orientation.[11,15,19,27,28] However, the extent of increase in these moduli and their relative values as loss factor (tan δ) depend on the type and strength of bonding between fiber and rubber. It was shown that weak interfacial bonding in the composite tends to increase the peak loss factor, whereas strong fiber–matrix adhesion decreases this factor.[19,28,29]

Many researchers in the field of rubber composites and tires have tried to understand the chemical and physical relationships that affect traction, wear resistance, and rolling resistance of tires.[30] They have shown that these characteristics of tires are not independent of one another because they are related through tire tread compound, a major viscoelastic hysteretic part of tires.[30,31] Reduction of rolling resistance and increasing traction while maintaining wear resistance of tires has been the objective of tire designers and rubber compound engineers.[32–34] Although there are numerous works on the properties of short fiber–rubber composites, few studies in the literature focus on the effect of short fibers on the properties of tire tread compounds. Some of these studies are available in the form of patents.[32–34] In one study, replacing part of carbon black, a major source of dissipation in rubber compounds, by aramid short fibers could produce low hysteresis truck tires,[35] but the direct effect of aramid short fibers on viscoelastic properties of tread compounds without reduction of carbon black was not discussed. Another advantage of using aramid short fibers in tire tread has been mentioned as increasing tire chunk resistance.[36] The effect of glass and carbon short fibers along with reinforcing sand on the properties of tire tread was studied, and the increase in coefficient of friction and abrasion resistance was observed.[17]

It is an industry accepted practice in tire performance prediction to use loss factor (tan δ) of the tread compound, measured in the laboratory as a predictor of tire traction and rolling resistance.[32–34] Normally, the rolling resistance of tread compounds has been evaluated in the laboratory under condition of 10 Hz frequency (approximate rolling tire frequency in service) and 50–80°C temperature range (approximate tread surface temperature in service). However, for tire treads sliding on rough road surfaces, the multi-scale asperities on the road apply high frequency dynamic loading on rubber.[37] Under this condition, dissipation of energy due to viscoelastic properties of bulk rubber compound has been recognized as the major contributor to rubber friction.[38] As a result, the coefficient of friction is considered a viscoelastic function of sliding speed and temperature which follows the Williams–Landel–Ferry (WLF) time–temperature shifting principle.[38] Therefore, high frequency asperity loading under service condition of tire tread has been replaced with lower frequencies and lower temperatures using the WLF principle for tire traction predictions in laboratories. As a common practice in tire industry, a frequency of 10 Hz and temperature range of **−20 to +5°C has been considered for this purpose.[32] A change in loss factor of about 0.005 has been considered large enough to be beyond experimental error, and changes of 0.015 and greater are significant and have clear effects on tire tread performances.[32] In the present work, tire tread compounds were processed in industrial scale, and effects of aramid short fiber addition and orientation on their mechanical, dynamic-mechanical, heat build-up, and wear resistance are discussed. Using loss-factor predictor, it is shown that the addition of aramid fiber in tire tread compound is in favor of both tire traction and rolling resistance while maintaining tire wear resistance.

EXPERIMENTAL

Materials

The reference rubber compound used in this study is a typical tire tread compound consisting of natural rubber (SMR-GP), polybutadiene rubber (Grade 1210) from Arak Petrochemical, carbon black from Ahvaz Carbon Black, aromatic oil from Behran Oil, and a conventional sulfur curing system. The recipes of the compounds are given in Table I. Aramid short fiber Technora-T323SB-DCF (Dipped Chopped Fiber) was provided by the Teijin-Twaron, Netherlands with average diameter of 12 μm. Physical-mechanical

TABLE I
Recipes of the Fiber-Filed Composite and the Reference Compound

Ingredients (part per 100 rubber)	Reference	Fiber-filled
Natural rubber, SMR20	80	80
High cis 1,4-polybutadiene (min. 97% cis)	20	20
Carbon black, N-330	38	38
Carbon black, N-660	5.0	5.0
Aromatic oil	8.0	8.0
Zinc oxide	4.0	4.0
Stearic acid	2.0	2.0
Antidegradant, 6PPD	2.0	2.0
Antidegradant, wax	2.5	2.5
Aramid short fiber, Technora DCF	0.0	1.0
Accelerator, TBBS	0.7	0.7
Sulfur	2.3	2.3

properties of technora aramid short fiber are given in Table II.

Processing

Mixing of the rubber compounds was performed in an industrial internal mixer Banbury-11D with 40 rpm rotor speed, followed by a two-roll-mill operation. All rubbers were added to the internal mixer and masticated for 1 min. The rest of ingredients including the aramid short fiber were added and mixing continued for another 4 min. The discharge temperature for this master batch (no curing system) from the internal mixer was about 160°C.

Milling after discharge from the internal mixer was performed on a 60″ length and 22″ diameter two-roll mill from Farrell for another 4 min in order to complete the mixing, cool-down the compound to about 60°C, and sheet it to slabs of about 2 cm thick. The continuous slab was sent through water-soap bath followed by a batch-off system to cool-down the slab to room temperature and collect it for further use.

After 24 h of aging, the compound was warmed up on another 60″ two-roll mill and hot-fed to a single screw extruder with 150 mm screw diameter and length to diameter ratio of 8 : 1 in order to extrude a tread slab with 160 mm width and 8 mm thickness in order to orient the short fiber in the rubber matrix in the direction of extrusion (longitudinal), as shown schematically in Figure 1. The process was performed at three screw speeds of 35, 40, and 45 rpm, at a temperature of 70°C at the hopper zone, at temperatures of 80, 90, and 90°C at two barrel zones and at the die, respectively.

Testing

The Mooney viscosity and curing rate of the compounds were measured with Monsanto MDR2000 (ASTM-D1646) and ODR2000 (ASTM-D2084) at 100°C and 140°C, respectively. Toluene was used as solvent for swelling experiments at 25°C for 72 h until equilibrium swelling was reached. Three disc-shaped specimens with diameter of about 30 mm and thickness of about 3 mm were punched from sheets and tested for swelling experiments.

Tensile testing was carried out in an Instron-5567 tester according to ASTM-D412. The number of specimens for each sample was three. The hardness was measured with a hardness tester Zwick D-7900 with a shore A durometer according to ASTM D2240 on three specimens of each sample.

Dynamic-mechanical-thermal (DMTA) properties were measured on a Tritic2000 analyzer from Triton company in a single cantilever bending mode at a frequency of 10 Hz, strain of 0.15%, and temperature range of −120 to +120°C. at a heating rate of 5°C/min (ASTM E-1640). The experiment was repeated twice for each sample.

Scanning electron microscopy (SEM) on cryogenically fractured and gold spotter coated surfaces was performed using a Phillips XL30 with an accelerating voltage of 20 kV. Heat build-up measurements were performed using a Doli Compression Flexometer under 4.45 mm displacement at 1800 rpm dynamic loading and in a heating chamber at 100°C according to ASTM D623. Finally, a Pico Abrader from Fortuna–Werke was used to measure the abrasion resistance of rubber compounds under 4.5 kg load and 60 rpm blade abrader rotational speed according to ASTM D2228.

RESULTS AND DISCUSSIONS

Degree of orientation

Swelling in the reference rubber compound with no fiber is isotropic as depicted in Figure 2(a), whereas rubber composites containing oriented fibers have anisotropic properties and will swell less in the direction of fiber orientation, as shown in Figure 2(b), schematically. Swelling experiments showed that the final dimension (diameter) of the swollen reference compound is about 49% and 50% larger than its original dimension in longitudinal and transverse directions, respectively. Linear swelling

TABLE II
Physical-Mechanical Specifications of the Technora DCF Aramid Short Fiber

Average L/D	250
Average fiber length (mm)	3
Tensile modulus (GPa)	20–21
Tensile strength (MPa)	3000–3250
Elongation at break (%)	5–7
Dipping material	Resorcinol formaldehyde latex (RFL)

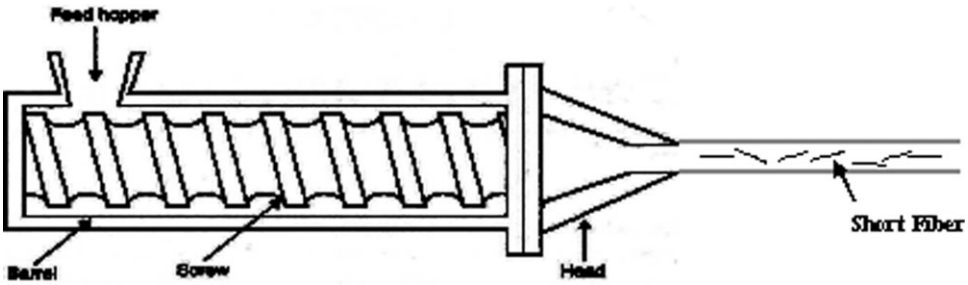

Figure 1 Schematics of the extruder and fiber orientation in the extruded rubber slab.

ratio has been defined as the ratio of swollen dimension to the original dimension.[12] Anisotropy in swelling of the fiber-reinforced specimens can be used as a measure of fiber orientation, and the degree of anisotropy can be defined as the difference in swelling ratios in longitudinal and transverse directions. Table III shows the mean and the standard deviation from the mean for swelling ratio as well as the degree of anisotropy for specimens extruded with different extrusion rates. These results were obtained by using three specimens for each sample. Reduction in swelling in the orientation direction with respect to the transverse direction can be attributed to lower segmental mobility of rubber chains due to higher frictional forces exerted by the fibers oriented in this direction. Small standard deviations for swelling ratio indicate reproducibility of the experimental procedure and meaningfulness of the evaluated degree of anisotropy. As this table shows, increasing screw speed from 35 rpm to 40 rpm enhances the degree of anisotropy, thus fiber orientation, which can be attributed to higher shear rates. However, further increase in screw speed to 45 rpm reduces the orientation of fibers, probably due to the turbulence flow in the extruder at high shear rates. Further studies on the properties of rubber composites are performed on the specimens with the highest degree of anisotropy processed with 40 rpm screw speed in this study.

Fractured Surfaces of the Composites

To observe orientation and adhesion of fibers to the rubber matrix qualitatively, SEM micrographs were obtained from the cryogenically fractured surfaces of rubber composites. These are shown in Figure 3(a–d). Figure 3(a,c) is obtained from the fractured planes perpendicular to the longitudinal and transverse directions at lower magnifications (order of 100×**), respectively. They clearly show the orientation of fibers occurred in the longitudinal direction during the process of extrusion. Presence of holes in Figure 3(a) is an indication of fiber-pull-out mechanism before fiber breakage due to very high strength of aramid fibers compared with not very strong fiber–rubber bonds. These holes are rarely seen in Figure 3(b) because the fibers are not pulled out of the matrix when the fracture process is occurred in the transverse direction (perpendicular to the direction of fiber orientation). Figure 3(b,d) is from the same fractured surfaces but at higher magnifications (order of 1000×) in order to observe the adhesion of fibers to the rubber matrix. As mentioned above, fibers lose their adhesion to the rubber matrix when fracture causes fiber pull-out. This can be seen from Figure 3(b) as loose fiber base after fibers are stretched from their place. Because Figure 3(d) is taken from a fractured plane perpendicular to the transverse direction, the process of fracture does not pull the fibers out of the matrix, and a proper adhesion of fibers to the matrix is due to bonds between the resorcinol formaldehyde latex (RFL) coating of fibers and the rubber can be observed from the proximal end of the fibers buried in the matrix in this case. SEM figures also show that the diameter of the fibers is about 12 μm, as already reported by the manufacturer.

Mechanical properties

Results of the uniaxial tension experiment and hardness measurements for the reference compound as well as the composites containing aramid short fibers, stretched in both longitudinal and transverse directions, are summarized in Table IV. The values of mean and standard deviations from the mean for

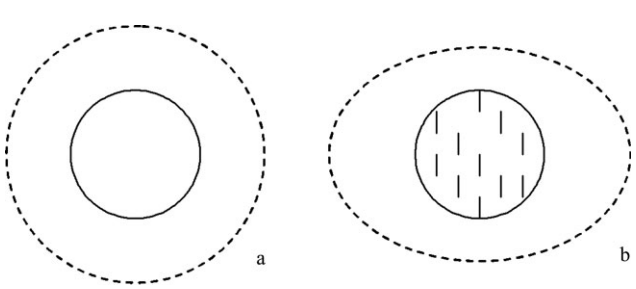

Figure 2 Schematics of rubber specimens before (solid circle) and after (dashed curve) swelling for (a) a compound with no fiber (b) a compound with oriented short fibers (solid lines).

TABLE III
Swelling Ratio and Degree of Anisotropy for the Vulcanized Fiber-Filled Composite and the Reference Compound with No Fiber Extruded under Different Screw Speeds

Specimen results	Reference	Fiber-filled 35 rpm	Fiber-filled 40 rpm	Fiber-filled 45 rpm
Swelling ratio, S_M (machine direction)	1.49 (0.0062)	1.416 (0.0087)	1.384 (0.0055)	1.396 (0.0082)
Swelling ratio, S_T (transverse direction)	1.50 (0.0060)	1.432 (0.0088)	1.446 (0.0090)	1.430 (0.0087)
Degree of anisotropy, S_T–S_M	0.01	0.016	0.062	0.034

The values in brackets are standard deviation.

three specimens of each sample are included in this table. As it can be seen from the results, orientation of fibers increases the modulus (at 300% strain) of the composite stretched in the longitudinal direction compared to that for the reference compound. Tensile strength and elongation at break for the fiber-reinforced composite in both cases of machine and transverse directions are slightly lower than those for the reference compound. Reduction of tensile strength in low loading of short fibers in carbon black filled rubber was attributed to dilution of particulate fillers in these composites,[1,8,14,15] however the extent of reduction is not as much to imply weakness of the fiber reinforced composite as a tire tread compound. Reduction of elongation at break in fiber-reinforced composite is an indication of bonding between fibers and rubber matrix.[15] Small standard deviations from the mean values given in this table are indication of meaningfulness of the results. Considering standard deviations for tensile strength of the fiber-filled composite stretched in both directions, one can conclude that there is not much difference in this property as a result of fiber orientation in low fiber loadings. However, due to higher modulus of the composite stretched in longitudinal direction, the value of elongation at break is slightly lower in this case. Addition of short fibers increases the hardness of the composite relative to the reference compound which is again an indication of adhesion between aramid fiber and rubber.

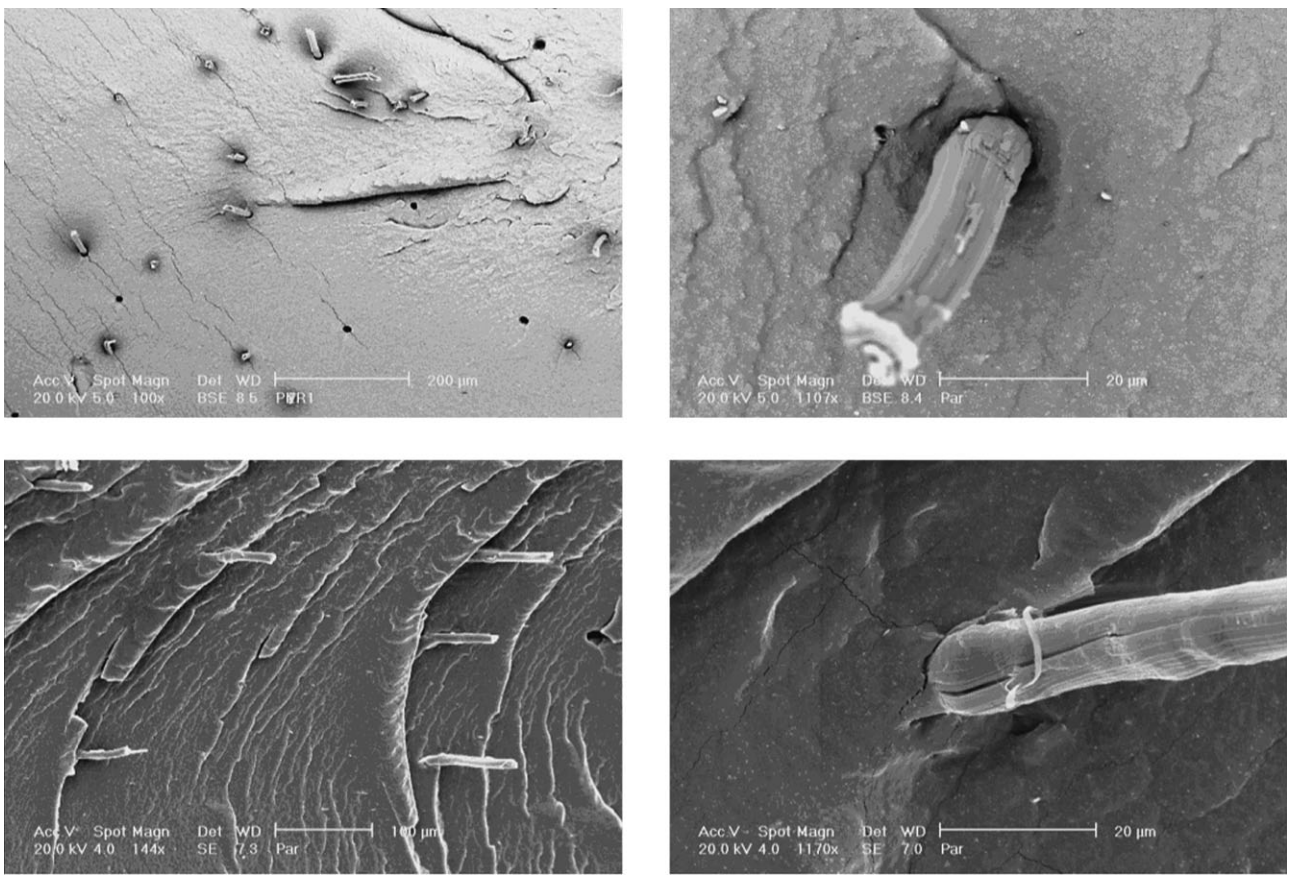

Figure 3 SEM micrographs of cross-sections perpendicular to longitudinal (orientation) direction (a, b) and transverse direction (c, d) at two different magnification orders (O100×, O1000×).

TABLE IV
Mechanical Properties of the Fiber-Filled Composites and the Reference Compound

Specimen results	Reference	Longitudinal direction	Transverse direction
Modulus @ 300% strain (MPa)	12.45 (0.07)	13.24 (0.07)	12.23 (0.08)
Tensile strength (MPa)	17.78 (0.44)	15.46 (0.55)	15.50 (0.77)
Elongation @ break (%)	409.21 (8.06)	355.52 (11.68)	371.51 (10.02)
Hardness (shore A)	66 (0.0)	70 (0.0)	70 (0.0)

The values in brackets are standard deviation.

DMTA

Results of DMTA experiments performed on the reference compound and the fiber-reinforced composites in both longitudinal and transverse directions are shown in Figure 4(a–c). Storage modulus (E') for the three cases is compared in Figure 4(a). It can be seen that storage modulus of the fiber-reinforced composite in the orientation direction has the highest value in the whole temperature range, followed by the storage modulus of the fiber-reinforced composite in the transverse direction and that of the reference compound, respectively. In the whole temperature range (see also the magnified graph), storage modulus of fiber-reinforced composite in the longitudinal direction is almost twice that for the reference compound at small strain of 0.15%. Enhanced orientation and reduction of molecular mobility of rubber chains in the longitudinal direction and local strain amplification in the rubber at the interface of rubber–fiber can be considered as the causes for increase in elastic storage modulus in this direction. These are all effective when there is enough bonding between rubber and the fiber surface. This effect is less pronounced when the composite is tested in the transverse direction. Figure 4(b) depicts the results of loss modulus (E'') for the same cases. A peak and a shoulder at about -47°C and -80°C correspond to glass transition temperature for natural rubber and butadiene rubber in the filled and vulcanized compound, respectively. This figure shows that E'' for the fiber-reinforced composites is higher than that for the reference compound before the polymer blend enters the full rubbery region. In the rubbery region, there are small differences among values of E'' for the three cases shown on the magnified graph, although E'' for the composite stretched in the longitudinal direction is still slightly higher. Molecular friction due to adhesion between rubber and fiber surface dissipates the work performed to slide the chains on the surface of fibers and adds up to the dissipating mechanisms already exist due to molecular friction among rubber chains. When polymer chains are rigid in the glassy state, deformational energy dissipates as frictional energy due to slippage of rubber chains on each other as well as on the surface of fibers. However, flexible chains in the rubbery state deform easily under the load and their sliding on the surface of fibers reduces. Small differences among values of E'' in the rubbery region hints on limited slippage of polymer chains on the fiber surfaces when polymers enter this region of the blend. Particulate fillers such as carbon black also increases frictional dissipation due to rubber sliding on the filler surface,[39] and it also increases the hysteretic behavior of the compound to a large extent, mostly due to filler agglomeration and networking, where the later mechanisms are absent in short-fiber reinforcement of rubber. As mentioned earlier, loss factor (tan δ) as the normalized loss modulus with respect to storage modulus (E''/E'), in other word "load-control" loss modulus, has been used to predict tire tread characteristics such as rolling resistance and traction during "load-control" service of tires.[32–34] Figure 4(c) shows the result of loss factor for three cases as a function of temperature. First of all, there is a slight shift of loss factor peak to higher temperatures as a result of fiber addition, especially for the composite tested in the longitudinal direction (about 1.2–2.0°C). This is an indication of immobilization effect of fibers on rubber chains due to adhesion between rubber and fiber. However, small temperature shift indicates that the number and strength of bonds are low in this case[12] which allows for rubber chain slippage on the surface of fibers. Also, the figure shows that there are two (lower and upper) crossover points where the order of loss factor values for the fiber-reinforced composites and the reference compound changes. Between these two points, especially from the peak position up to the upper crossover point, the loss factor for the fiber reinforced composite in both longitudinal and transverse directions is higher than that for the reference compound. This predicts a higher traction for the fiber reinforced composite as a result of additional dissipating mechanism of rubber–fiber slippage. The upper crossover temperature is not a fixed point in repeated experiments, and it occurred in a temperature range of -3°C to about $+3$°C. On the other hand, above the upper crossover point, especially in the service temperature of tire tread (40–100°C) as shown in the magnified graph, the value of loss factor for the fiber-reinforced

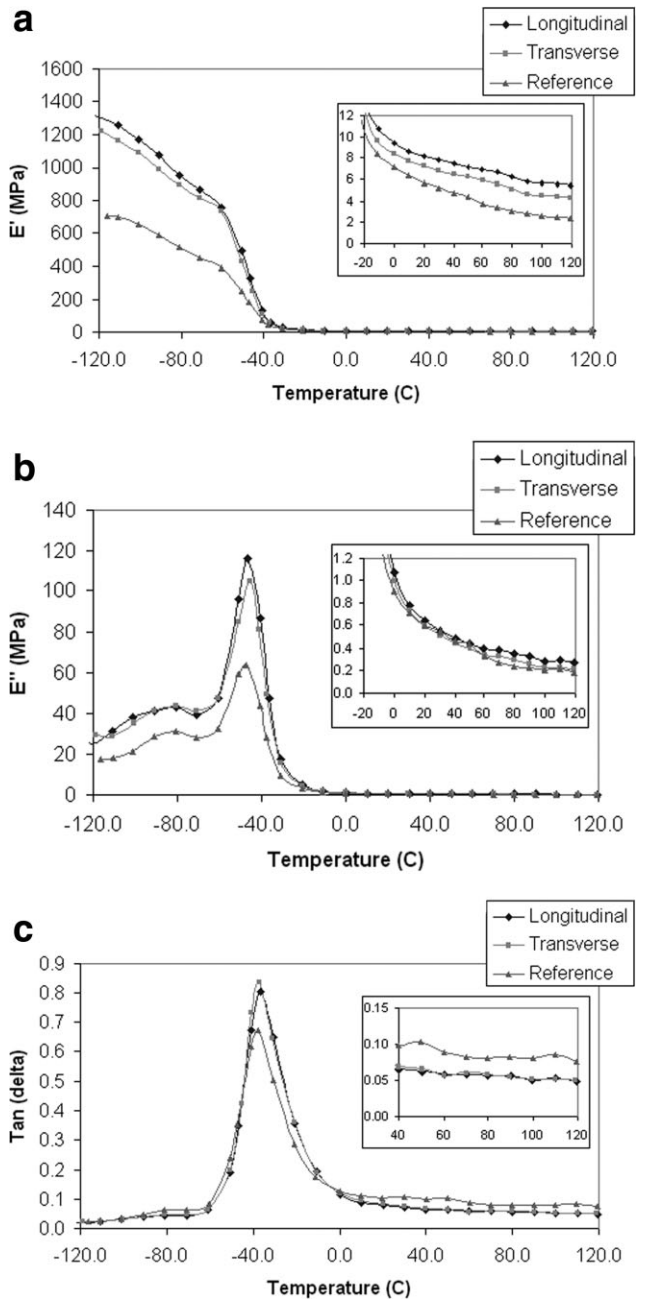

Figure 4 DMTA results for the fiber-filled composites and the reference compound. (a) storage modulus (b) loss modulus (c) loss factor.

composite tested in both directions is smaller than that for the reference compound. This is due to larger differences between storage modulus of the composites and the reference compound compared with the differences in their loss modulus in this temperature range, as seen in the magnified graphs of Figure 4(a,b). This significant change in loss factor (more than 0.02) predicts lower rolling resistance for the composite than the reference compound with no fiber. According to the loss factor predictor in this study, one part aramid short fiber has the potential to increase tire traction up to 35 ± 5% (at −20°C) and decrease rolling resistance of tires up to about 29 ± 3% (at +80°C).

The Goodrich heat build-up

Similar to DMTA, the Goodrich heat build-up experiment is performed under "displacement-control" condition. Results of these experiments are shown in Figure 5. Considering error bars in this figure, it can be noticed that the fiber-reinforced composite tested in the longitudinal direction has the highest heat generation value among three samples, but there is no meaningful difference between the composite tested in transverse direction and the reference compound. These results agree well with the results obtained for the loss modulus (E'') under displacement-control condition at about 100°C in Figure 4(b). Although fiber orientation causes higher heat generation under the displacement-control condition, this might be misleading for the tire tread compound performing under a defined load during its service, as discussed earlier. Therefore, to predict heat build-up in tire treads under service conditions, it is more profitable to use loss factor as a measure of energy loss and rolling resistance.

Abrasion resistance

Results of abrasion loss for the fiber-filled composite and the reference compound obtained from the Pico abrasion test are depicted in Figure 6. These are the average of four specimens for each sample. The fiber-reinforced composite was tested in the plane of fibers (longitudinal-transverse). Considering error bars in this figure, one can notice that there is no meaningful difference in abrasion of the fiber-filled composite and the reference compound. This result predicts that addition of one part aramid short fiber will not deteriorate the abrasion resistance of tread

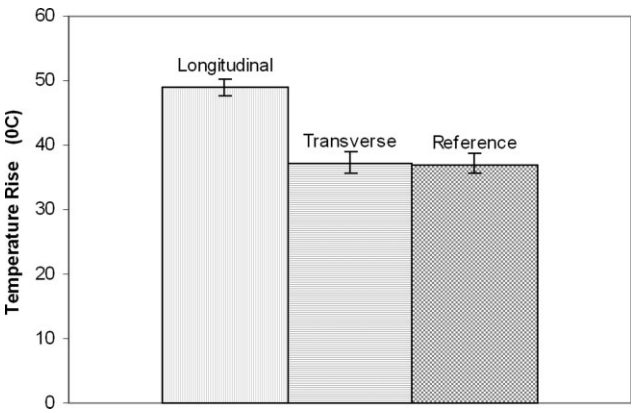

Figure 5 The Goodrich heat build-up for the fiber-filled composites and the reference compound.

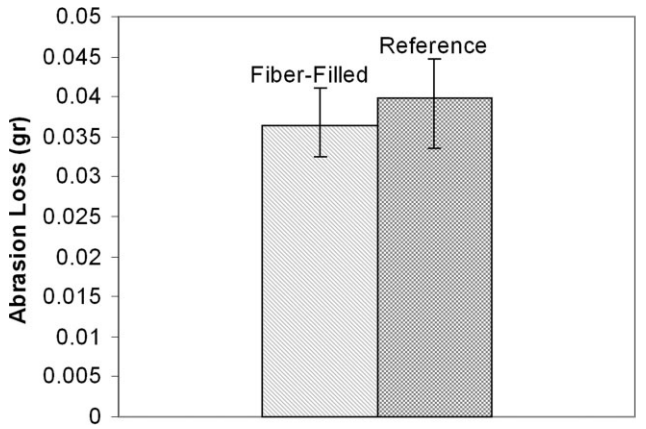

Figure 6 The Pico Abrasion for the fiber-filled composite and the reference compound.

compounds. As mentioned earlier, the objective of tire designers is to decrease rolling resistance and increase traction while maintaining the abrasion resistance of tires.

Processing and vulcanization Characteristics

In order to study the effect of aramid short fibers on processing and vulcanization characteristics of tire tread compounds, Mooney viscosity, reactive torque, and vulcanization times of the fiber-reinforced composites were compared with those of the reference compound in Table V. As this table shows, the Mooney viscosity (ML @4′), minimum torque (ML), and maximum torque (MH) have slightly increased in the fiber-reinforced composite compared to that for the reference compound with no fiber. However, the vulcanization times (TS2, T50, T90) of two compounds are almost the same. Therefore, it can be concluded that addition of one part of aramid fibers to this typical tire tread compound did not affect processing and vulcanization characteristics of the compound measured in the laboratory to a great extent.

CONCLUSIONS

One part aramid short fiber was mixed in a typical tire tread compound, and the mixture was extruded in an industrial scale to study the degree of fiber orientation in the tread extruded profile. Fiber orientation was assessed by the degree of anisotropy obtained by the swelling method, quantitatively. Also, the SEM of the fractured surfaces revealed orientation of fibers in the longitudinal direction and the mechanism of failure as fiber pull-out in the composites, qualitatively. This mechanism was attributed to strong strength of aramid fibers compared with lower strength of bonding between rubber and the RFL-coated fibers. Results showed that there is an optimum extruder screw speed of 40 rpm, which provides the highest degree of fiber orientation, thus anisotropy, in the extruder under processing conditions used in this study. It was shown that aramid short fibers can increase modulus and stiffness of the tread compound, but it slightly reduces the tensile strength and elongation at break in a uniaxial tension test, which has insignificant effects on mechanical characteristics of tire tread compounds. Dynamic viscoelastic studies on the vulcanized samples revealed that both storage and loss moduli for the fiber-reinforced composites were higher than those for the reference compound at the glassy region of the polymer blend. However, it was interesting to note that by entering the full rubbery region, the loss moduli of the composites become closer to, though still higher than, that for the reference compound while the storage modulus of both longitudinal and transverse directions remain higher than that for the reference compound to a greater extent. This was related to a limited sliding of rubber chains on the surface of fibers in the rubbery region compared with the glassy region. This leads to a temperature (or frequency) dependency for the relative values of loss factor in three measured cases. The loss factor for the composites was higher below a crossover temperature and lower above this temperature compared to that for the reference compound with no filler. According to industry accepted application of loss factor as a predictor of viscoelastic properties of vulcanized tread compounds, this significant change in loss factor predicts lower rolling resistance and higher traction for the tire tread compound containing only one part of aramid short fiber. Results of the Goodrich heat-build up agree well with the trend of high-temperature loss modulus obtained from dynamic properties, but it can not be used as a predictor of rolling resistance. The Pico abrasion test showed that abrasion resistance of the fiber-reinforced composite is close to that of the reference compound. This proves that slight reduction of tensile strength in the fiber-reinforced composites does not have any adverse effect on

TABLE V
Processing and Cure Characteristics of the Fiber-Filled Composites and the Reference Compound

Specimen results	Reference compound (no fiber)	Fiber-reinforced composite
Mooney viscosity ML 4′ @100°C (MU)	42.3	44.4
Minimum torque ML (N m)	0.48	0.56
Maximum torque MH (N m)	3.61	3.82
Scorch time TS2 (min)	2.65	2.70
Cure time T50 (min)	4.17	4.44
Cure time T90 (min)	6.77	6.88

failure mechanisms such as rubber abrasion. Finally, the Mooney viscosity and vulcanization times of both compounds are close enough to assure that no significant change in processing and vulcanization characteristics of the tread compound as a result of aramid short fiber addition.

The author thanks Iran-Tire Manufacturing, for their help and support in providing material, equipment, and laboratory instruments throughout this project. Also, the author is grateful to Persiamid for providing aramid short fibers from Teijin-Twaron for this study.

References

1. Goetler, L. A.; Shen, K. S. Rubber Chem Tech 1983, 56, 619.
2. Goettler, L. A. In Short Fiber-Rubber Composites, Handbook of Elastomers, New Developments and Tech., Bhowmick, A. K.; Stephens, H. L., Eds.; Marcel Dekker, Inc: New York, 1988; p 215–248.
3. Goettler, L. A.; Sezna, J. A.; DiMauro, P. J. Rubber World 1982, 187, 33.
4. Foldi, P. Rubber World 1987, 196, 19.
5. Schuller, T.hF. Internationale Kautschuk-Tagung 1991, 27, 41.
6. Prevorsek, D. C.; Kwon, Y. D. Rubbercon 92.
7. Goettler, L. A. Polym Compos 1984, 5, 60.
8. Sreeja, T. D.; Kutty, S. K. N. J Elast Plast 2001, 33, 225.
9. Sreeja, T. D.; Kutty, S. K. N. J Elast Plast 2002, 34, 157.
10. Sreeja, T. D.; Kutty, S. K. N. Int J Polym Mater 2003, 52, 239.
11. Webber, M. E.; Kamal, M. R. Polym Compos 1992, 13, 133.
12. Ibarra, L.; Chamorro, C. J Appl Polym Sci 1991, 43, 1805.
13. Das, B. J Appl Polym Sci 1973, 17, 1019.
14. Abdel-Bary, E. M.; Eman, W.; El-Nesr, M.; Helaly, F. M. Polym Adv Technol 1997, 8, 140.
15. Vajrasthira, C.; Amornsakchai, T.; Bualek-Limcharoen, S. J Appl Polym Sci 2003, 87, 1059.
16. Abdelmouleh, M.; Boufi, S.; Belgacem, M. N.; Dufresne, A. Compos Sci Technol 2007, 67, 1627.
17. Rios, S.; Chicurel, R.; Del Castillo, L. F. Mater Des 2001, 22, 369.
18. Geethamma, V. G.; Mathew, K. T.; Lakshminarayanan, R.; Thomas, S. Polymer 1998, 39, 1483.
19. Geethamma, V. G.; Kalaprasad, G.; Groeninckx, G.; Thomas, S. Compos Part A: Appl Sci Manuf 2005, 36, 1499.
20. Prasantha Kumar, R.; Manikandan Nair, K. C.; Thomas, S.; Schit, S. C.; Ramamurthy, K. Compos Sci Technol 2000, 60, 1737.
21. Martins, M. A.; Mattoso, L. H. C. J App Polym Sci 2004, 91, 670.
22. Lovely, M.; Rani, J. J App Polym Sci 2007, 103, 1640.
23. Hanafi, I.; Edyham, M. R.; Wirjosentono, B. Polym Test 2002, 21, 139.
24. Lopez Manchado, M. A.; Arroyo, M. Polym Compos 2002, 23, 666.
25. Prasantha Kumar, R.; Geethakumari Amma, M. L.; Thomas, S. J Appl Polym Sci 1995, 58, 597.
26. Mathew, L.; Joseph, R. J Appl Polym Sci 2006, 103, 1640.
27. Saikrasuna, S.; Amornsakchaia, T.; Sirisinhaa, C.; Meesirib, W.; Bualek-Limcharoena, S. Polymer 1999, 40, 6437.
28. Rajeev, R. S.; Bhowmick, A. K.; De, S. K. Polym Compos 2002, 23, 574.
29. Kutty, S. K. N.; Nando, G. B. J Appl Polym Sci 1991, 43, 1913.
30. Tires and Passenger Vehicle Fuel Economy-TRB Special Report, 286 2006.
31. Pan, X.-D. Wear 2007, 262, 707.
32. Gatti, L., World Intellectual Property Organization PCT/US99/08838, 1999.
33. Palombo, J. L.; Miller, R. L. United Stated Patent 4675349, 1987.
34. Scriver, R. M. European Patent Application EP0359693A1, 1989.
35. Data, R. N. 165th ACS Rubber Division Meeting, Paper 26.
36. Data, R. N. Rubber & Plast News 2004, 10, 18.
37. Persson, B. N. J. Surf Sci 1998, 401, 445.
38. Grosch, K. A. Proc R Soc, Lond A 1963, 274, 21.
39. Dannenberg, E. M. Rubber Chem Technol 1975, 48, 410.